International Journal of Adhesion & Adhesives 116 (2022) 103153

Contents lists available at ScienceDirect

International Journal of Adhesion and Adhesives

journal homepage: www.elsevier.com/locate/ijadhadh

Impact of the processing method on the properties of castor oil/cellulose acetate polyurethane adhesives for bonding wood

Adrián Tenorio-Alfonso *, M. Carmen Sánchez, José M. Franco

Pro²TecS-Chemical Product and Process Technology Research Centre, University of Huelva, 21071, Huelva, Spain

ARTICLE INFO

Keywords:
Cellulose acetate
Castor oil
Green chemistry
Solvent-free synthesis
Bio-sourced adhesive

ABSTRACT

During the last decades, the replacement of the traditionally petro-based raw materials by eco-friendly substances in polyurethane production has become a great challenge. The synthesis of polyurethanes is mainly conducted by means of a selective reaction between active isocyanate and hydroxyl groups, yielding a characteristic segmented chemical structure. In this study, the traditional solvent-based polycondensation reaction for the synthesis of bio-based polyurethane adhesives, involving first cellulose acetate modification with 1,6-hexamethylene diisocyanate and subsequent crosslinking with castor oil, was evaluated and compared with a simpler solvent-free single-step protocol. The impact of the preparation procedure and reagent proportions, on the chemical structure, thermo-rheological behaviour and ultimate adhesion performance were evaluated. The rheological response and adhesion performance of these bio-inspired polyurethanes were also compared to those found in some commercial adhesives. This research highlights the reinforcing and stabilizing effect of cellulose acetate on bio-polyurethane performance. Particularly, the inclusion of cellulose acetate into the adhesive manufacture allowed a reduction in the maximum curing time under room conditions to almost one week, while yielding a higher thermal stability and a fourfold increase in elastic modulus in comparison to the cellulose acetate-free counterpart. Moreover, the proposed solvent-free synthetic route enhanced the microphase mixing of the ensuing bio-based polyurethanes, exhibiting an adhesion performance comparable to the considered commercial benchmarks, but with failure occurring primarily within the substrate material – the preferred locus of failure.

1. Introduction

Wood materials have emerged as one of the main sources for the construction industry, due to their insulating and aesthetic characteristics, besides the low environmental impact, they may entail. Nevertheless, in order to develop timber constructions, wooden pieces demand the application of joining techniques, including the use of polymer-based adhesives which have proven effective in joining wood materials [1] since they allow the ability to distribute stresses evenly along the whole bonding line and reduce the weight and production costs of bonded products [1,2]. In the last century, worldwide adhesive annual consumption amounted to 14 Mt, and it is thought to continue to grow by almost 4% per year in the next decade, according to the worldwide market study conducted by Ceresana [3].

Since the advent of polymer adhesives, their production sharply hinged on conventional crude oil, leading to the production of the well-known solvent-borne adhesives, responsible for the release of volatile organic compounds (VOCs) during both, processing and application of these adhesives [4]. Therefore, the development of green adhesives for bonding wood, in pursuit of alternatives to traditional hazardous raw materials, has arisen as a prevailing environmental and economic commitment [5]. In particular, polyurethanes (PUs) have been generally considered as a promising choice for wood-joints, since the ultimate adhesion response relies not only on physical interactions but also on chemical bonding between active isocyanate and pendant hydroxyl groups of the lignocellulosic substrates [6].

It is universally acknowledged that PU synthesis is traditionally accomplished by the so-called polyaddition reaction, in which a reaction between hydroxyl (OH) and isocyanate (NCO) group bearing compounds (polyols and polyisocyanates) is promoted with the aid of chain extenders and catalysts [7], producing carbamate linkages, typically urethanes (NHCOO). Sensible modifications in molecular weight, branching, or chemical structure of the reagents, in general, as well as the NCO:OH ratio, may result in substantial changes in ultimate

* Corresponding author.
E-mail address: adrian.tenorio@diq.uhu.es (A. Tenorio-Alfonso).

https://doi.org/10.1016/j.ijadhadh.2022.103153

Available online 24 March 2022

polyurethane properties and, hence, in its application fields [8]. Such tunability is derived from the complex two-phase conformation, characterised by wanting thermodynamic compatibility of both microdomains, namely soft (SS) and hard segment (HS) blocks [9]. Soft and hard segments, coming from the original polyol and polyisocyanate-chain extender backbones respectively, can eventually compete for the formation of hydrogen bonds in a variety of ways (HS···HS, SS···HS, etc.), giving rise to a certain degree of microphase separation in the polymer network, which, in turn, results in an enhancement in the mechanical properties of the polyurethanes [10,11].

Furthermore, as Cui et al. [12] reported, as a consequence of the apparent limitations when searching for sustainable biomaterials containing active NCO functional groups, the assessment of the likely natural alternatives to replace the former petrochemical polyols has been in the spotlight of the research in recent years. Natural sources including lignocellulosic materials [13], vegetable oils [14], proteins [15], agricultural wastes [16,17], etc … have been lately proposed for PU synthesis, aiming to reduce the environmental impact and energy consumption.

Cellulose, together with its different derivatives, constitutes a natural hydroxyl-rich source. Their high availability, renewability, high reactivity with isocyanates and noticeably low environmental burden makes these biomaterials especially appealing for polyurethane production [18]. Similarly, vegetable oils have drawn the attention for greener adhesive development, on account of their good functionality, technical versatility, large abundance and cost-effectivity [14], so that at the beginning of the 21st century an extensive spectrum of vegetable oils such as palm [9,19], soybean [15,20,21], jatropha [22] or castor [5,14,23] oils, have been used to manufacture bio-based PU adhesives.

Castor oil (CO) is a non-food grade natural feedstock obtained from *Ricinus communis* seeds [24]. Due to the fatty acid lengths and the particular arrangements of pendant chains in their structure [25], hampering the penetration of foreign substances, CO-based polyurethanes present improved thermo-mechanical stability in combination with chemical and water resistance [4,26]. Moreover, its particularly high unsaturation degree, along with the fact that castor oil belongs to the limited group of hydroxylated plant oils, empowers it to suitably take part in the industrial production of polyurethanes [5,13]. Indeed, a wide variety of studies have been carried out promoting the development of castor oil-based PUs with apparent adhesion properties. More specifically, Fonseca et al. [27] described the production of CO-based PU adhesives by developing chain extenders via self-metathesis synthesis. Moghadam et al. [5] in their research reported a simple procedure in line with the fundamentals of green chemistry to synthesize wood adhesive PUs from modified castor oil, whose lap shear strengths appeared to surpass the analogous benchmark. Patel et al. [28] proposed the modification of castor oil to develop natural polyols as feedstock for polyurethane with adhesive applications on wood and metal substrates. Bio-sourced PUs obtained by Sahoo et al. [14], when evaluating the influence of the NCO:OH molar ratio, exhibited adhesion strength values almost fourfold greater than the commercial benchmark. Finally, in our previous investigations, adhesives from NCO-functionalized cellulose acetate and castor oil were synthesized [29], and compared with a wide spectrum of commercialized adhesives, resulting in similar or even improved adhesion response on wood and stainless-steel surfaces, in conjunction with a significantly higher elasticity [30].

Castor oil has usually undergone different chemical modification processes to yield polyols, possessing higher hydroxyl content and ready availability [27]. The functionalization routes most frequently applied comprise transesterification [5], along with epoxidation [31]. However, these additional treatments imply the utilization of supplementary solvents, catalysts, or high temperatures and/or pressures which, according to the green chemistry tenets [32], could compromise the environmentally friendly character of the synthesis methodology inasmuch as an extra energy consumption arises from the requirement of a further removal of such substances from the adhesive system prior to application [10]. Besides, aiming to attenuate the impact of PU adhesives on the environment, it is required not only the replacement of hazardous raw materials and sources [33] but also some attention should be paid on the synthesis protocol [5,34].

In order to delve further into this concern, this study analyses the feasibility of a one-step solvent-free synthesis protocol for the development of a CO-based adhesives, in comparison to that applied in previous investigations [29,30]. This aims to simplify PU manufacture and avoid the use of solvents, catalysts, intermediate modifications, or complex reaction conditions thus, meeting to a larger extent the principles of green chemistry. Thence, bio-sourced PU wood adhesives were processed from mixtures of cellulose acetate, castor oil and 1,6-hexamethylene diisocyanate, through two different preparation methodologies, double- and single-step protocols. The influence of the synthetic routes on the adhesion performance, chemical structure and thermal and rheological properties of the resulting polyurethanes was analysed.

2. Materials and methods

2.1. Materials

Castor oil (211 cSt at 40 °C) was furnished by Guinama (Valencia, Spain) and used in its original form. Cellulose acetate ($M_n \sim 30000$, 40% acetyl groups) and 1,6-hexamethylene diisocyanate (purity ≥98.0%, boiling point: 82–85 °C/0.1 mmHg), hereinafter CA and HMDI respectively, were supplied by Sigma-Aldrich (St. Louis, MO, USA). All other solvents and catalysts were laboratory grade chemicals and obtained from Sigma-Aldrich (St. Louis, MO, USA). Furthermore, commercially available adhesives U-Bond® 309-TFC (C.Ad.1) and UHU® Montakit® (C.Ad.2) considered for benchmarking purposes, together with adhesion substrates, namely polyester fabric (PF), poplar wood (PW), spruce wood (SW), oak wood (OW), plywood (PlyW) and medium-density fibreboard (MDF) were provided by local stores.

2.2. Synthesis methods

The different methods considered in this study to prepare the bio-based PU adhesives can be detailed as followed:

Two-step protocol. This method matches the procedure well-described in previous investigations [29]. In principle, this two-step methodology aims to partially functionalize CA with HMDI intending to further promote the chemical interaction of CA and CO triglycerides more selectively. In the first stage, the modification of a certain amount (see Table 1) of pre-dried cellulose acetate with HMDI was performed in toluene in the presence of triethylamine catalyst. The reaction mixture was maintained under continuous stirring at 500 rpm for 24 h, at room temperature, and under an argon atmosphere. In a second stage, after removal of the solvent under vacuum, the NCO-terminated prepolymer was mechanically blended with castor oil in a 1:1 wt ratio at room conditions for 24 h. A selected proportion of the reagents was used in this synthesis protocol (Table 1). The influence of NCO-ended prepolymer to castor oil proportion, following this synthesis protocol, on the mechanical properties and adhesion performance of these adhesives

Table 1
Weight proportions of the components used in the preparation of natural-based PU adhesives.

Sample		Weights (g) per 100 g			NCO:OH ratio	Renewable content (% wt.)
		CA	HMDI	CO		
Two-Step	PU2	11.8	38.2	50	1.87	61.8
Single-Step	PU1a	11.8	38.2	50	1.87	61.8
	PU1b	0	30.9	60.1	1.87	60.1
	PU1c	0	43.3	56.7	3.20	56.7

have been previously reported [29,30].

Single-step protocol. In this study, aiming to completely avoid the use of environmentally hazardous chemicals as solvents or catalysts, and to reduce the number of synthesis steps above outlined, a single step procedure was proposed. Three different PU adhesives were prepared by mechanically stirring different proportions of the reagents (Table 1), *viz.* CA, HMDI and CO, inside an opened reactor at 60–75 rpm, for 48 h at room temperature (~20 °C). Under these conditions no hazardous volatiles are expected, except for the likely CO_2 resulting from the humidity-driven curing process [35].

2.3. Characterization of PU adhesives

2.3.1. FTIR analysis

Fourier transform infrared (FTIR) spectra of the synthesized adhesives were acquired with a Jasco FT/IR-4200 spectrophotometer (JASCO Inc., Easton, MD, EEUU) fitted with an attenuated total reflection (ATR) apparatus. The measurements were performed at room conditions by using a monolithic diamond crystal as a prism, with an incidence angle of the laser beam of 45°, with 4 cm^{-1} of spectral resolution. Infrared spectra were recorded after 100 scans, over the spectral range from 4000 to 650 cm^{-1} with the aid of the Spectra Manager software. The progress of the curing process was followed by monitoring the decrease of the peak area attributable to the free isocyanate functional group (-NCO), 2261 cm^{-1}. Upon completion of the curing process (14–24 days, depending on the PU system), the same FTIR analysis, also including the application of the deconvolution methodology over the carbonyl region (1770-1600 cm^{-1}) of the fully cured bioadhesives was performed.

2.3.2. Thermal characterization (TGA and DSC)

The thermal stability of PU adhesives resulting from the proposed protocols was assessed by carrying out thermogravimetric analysis (TGA). Approximately 10 mg of PU samples were placed in open aluminium crucibles and submitted to a heating ramp of 10 °C·min^{-1}, from 30 to 600 °C with a 60 mL min^{-1} flow of dry nitrogen purge, using a Thermogravimetric Analyzer Q50 (TA Instruments, New Castle, DE, USA). During the heating process, weight loss and decomposition rate were recorded as a function of temperature.

The thermal properties of the bio-sourced polyurethanes were analysed in a differential scanning calorimeter DSC250 (TA Instrument, New Castle, DE, USA). Hermetic aluminium pans loaded with 3–5 mg of cured polyurethanes were subjected to a heating cycle from −80 up to 300 °C, with a scan rate of 10 °C·min^{-1} under an inert purge of nitrogen (50 mL min^{-1}). However, as a consequence of the well-known limitations of standard DSC analysis, i.e., likely overlapping of several thermal transitions arising from the contribution of different constituents in the polymer network, temperature-modulated DSC (MDSC) analysis, also under nitrogen environment, was conducted by applying a heating rate of 2 °C·min^{-1}, in the range of 0–300 °C, with a modulation amplitude and period of 0.32 °C and 60 s, respectively [36]. TRIOS and Universal Analysis software were employed for the analysis.

2.3.3. Rheological characterization

The linear viscoelasticity response of the synthesized bio-inspired PU adhesives under torsional mode was evaluated and benchmarked against those adhesives already on the market by using a Physica MCR301 rheometer (Anton Paar, Graz, Austria). Completely cured bio-based PUs were submitted to a temperature ramp in the range from 25 to 200 °C (2 °C·min^{-1}, 1 Hz). Viscoelastic behaviour arising from the application of oscillatory deformation was also analysed, within the angular frequency region of 100-0.01 rad s^{-1}. With the objective of assessing the feasibility of the time-temperature superposition principal application, aimed to expand the mechanical spectra, frequency sweep experiments were accomplished at different temperatures (from 25 up to 200 °C). All the viscoelastic measurements were conducted in triplicate and carried out inside the linear viscoelastic range, previously established by applying stress amplitude sweeps throughout the whole temperature ranges considered.

2.3.4. Adhesion measurements

Peel testing at 180° and single-lap shear strengths of the studied adhesives were evaluated on a wide selection of wooden substrates (see section 2.1) by following the American standardized tests ASTM D903 and D906, respectively. All mechanical tests were conducted in an AG-IS Universal Testing Machine (Shimadzu, Kyoto, Japan), equipped with load cells with capacities of 1 and 10 kN, selected in accordance with the requirements of the strength to be measured. Before pouring the bio-based polyurethanes on the adhesion substrates, wooden samples and polyester fabric were gently wiped with acetone to remove likely impurities and oily compounds which may distort the bonding process. Upon spreading the just prepared adhesives, the thicknesses were set to 0.5 mm with the aid of silicon spacers (see Figure S 1), all the specimens were joined and allowed to cure at a relative humidity of 64% and ambient temperature. Single-lap shear strengths were calculated as the maximum stress (MPa) while peeling strengths were recorded as the average load per bonding width (kN/m). Overlap joint areas and test conditions are gathered in Table S 1. Finally, the sort of failures was reported as a result of a photographic assessment of the bonding areas subsequent to joint breakage.

Each adhesive specimen was evaluated ten times repeatedly, and the resulting data were submitted to a statistical analysis by conducting the Generalized Extreme Studentized Deviated (ESD) test, aimed to track down likely outliers with a level of significance of $\alpha < 0.05$. All the results are presented as the arithmetic mean and the corresponding standard deviation, after removing the outliers. Additionally, one-way ANOVA for the analysis of variance, together with a post-hoc test, was also performed, in order to establish statistical differences with an $\alpha < 0.05$ of the significance level.

3. Results and discussion

3.1. Structural analysis

The influence of the synthetic route on the developed polyurethane adhesives' chemical structure was approached by means of Fourier transform infrared spectroscopy in attenuated total reflection (ATR). Fig. 1 plots the results obtained for the two-steps polyurethane adhesive (PU2) when recording the evolution of the NCO asymmetric stretching vibration (2261 cm^{-1}) [29,37] over time, estimating the moisture-cure conversion (X^t_{NCO}) as follows [7]:

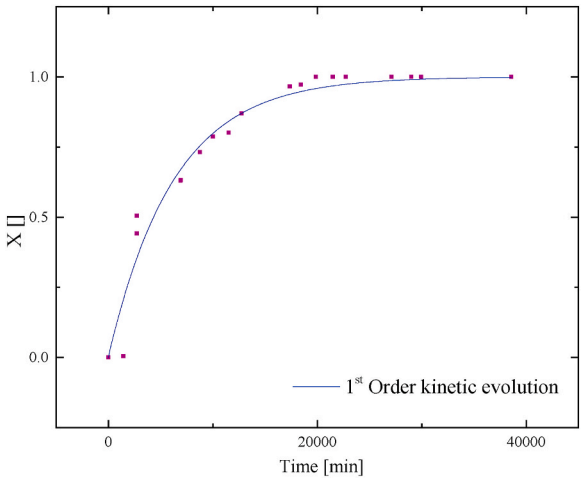

Fig. 1. Monitoring of the humidity-driven curing process for PU2 sample.

$$X^{t}_{NCO} = \frac{[A]^{t_0}_{NCO} - [A]^{t}_{NCO}}{[A]^{t_0}_{NCO}} \quad (1)$$

where the normalized areas assigned to leftover isocyanates at time *0* and *t* refer to parameters $[A]^{t_0}_{NCO}$ and $[A]^{t}_{NCO}$ respectively, taking as reference the peak associated with the carbohydrate backbone vibrational stretching (-CH_3/-CH_2, 2924 cm^{-1}).

Therefore, an approximate kinetic study of post-synthesis ageing was performed, assuming that the reaction with environmental humidity (see Fig. 2) was the predominant driving force for the free isocyanate consumption at stable conditions. The absence of the hydroxyl (-OH) characteristic peak centred at 3360 cm^{-1} during the first 30 min of curing for all bio-based polyurethanes (Fig. 3a), supports such an assumption. Although the well-known nucleophilic addition taking place between NCO and OH active groups is typically a second-order reaction [25], as can be inferred from Fig. 1, in this study the extent of the NCO conversion for all bio-sourced polyurethanes was well fitted to a first-order equation (2), whose resulting constant kinetics (*k*) are gathered in Table 2.

$$X^{t}_{NCO} = 1 - e^{-kt} \quad (2)$$

This reaction order may have arisen from the fact that, under the same curing conditions, any moisture dependence (i.e. [H_2O]) can be subtracted, since the limiting reagents were always the free NCO compounds. Furthermore, in terms of the reaction kinetics, the protocol optimisation (PU1a vs PU2) appears not to have brought about a significant impact on the curing rate. However, when analysing the influence of CA addition as an additional source of hydroxyl groups together with castor oil, CA-based polyurethane adhesives (PU2, PU1a), unlike the others (PU1b, PU1c), underwent a favoured curing process as can be concluded from the increase in the kinetic constants (Table 2). Thus, a higher castor oil content (PU1b and PU1c) may lead to lower kinetic constants, in other words, longer curing times.

On the other hand, IR spectra for all polyurethane adhesives upon completion of the curing stage are depicted in Fig. 3b. Regardless of the procedure or their composition, infrared absorption bands attributed to polyols and diisocyanate backbones can be identified, including stretching of alkene = C–H (3010 cm^{-1}), in-phase and out-of-phase motions of methyl (-CH_3) and methylene (-CH_2) groups (2924 and 2853 cm^{-1}), aliphatic carbonyl (C═O) band (1742-1748 cm^{-1}), C═C absorption (1645 cm^{-1}) and ester C–O vibration (1141-1216 cm^{-1}), as well as absorption of asymmetrical (1479 cm^{-1}) and symmetrical (1375 cm^{-1}) –CH_3 bending, and –CH_2 scissoring (1463 cm^{-1}) and rocking (723 cm^{-1}) [7,12,37,38]. Moreover, the production of secondary amides during the development of the natural adhesives was corroborated by the identification of their main absorption bands, such as N–H stretching and the amide regions I (C═O band), II and III (mixed contribution of C–N stretching and N–H bending vibrations), and IV (N–H out-of-plane) attributable to the peaks centred at 3325, 1600–1735, 1509–1580, 1337 and 773 cm^{-1} respectively [38,39].

Given the strong dependence of segmented-polyurethane properties on the microdomain distribution and interaction of soft and hard segments and bearing in mind the high sensitivity of the IR technique to the

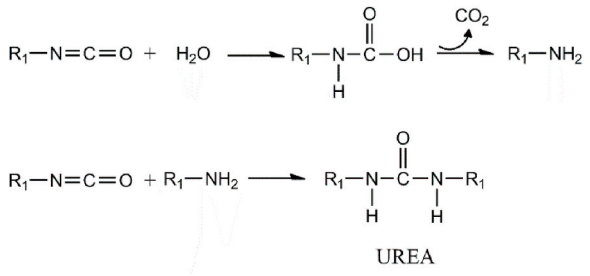

Fig. 2. Environmental moisture-curing process.

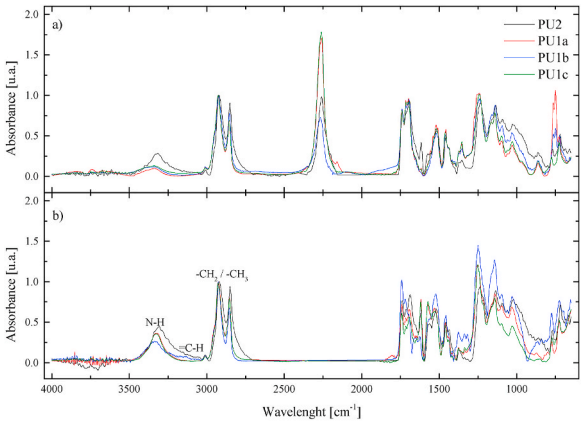

Fig. 3. FTIR Spectra for all PU adhesives at different times: a) during the early stages of the curing process and b) fully-cured adhesives.

Table 2
Kinetics constant and time needed for the completion of the moisture-driven curing process.

Sample	k [min^{-1}]	t_{Tot} [days]
PU2	$1.6{\cdot}10^{-4}$	14
PU1a	$1.4{\cdot}10^{-4}$	19
PU1b	$8.5{\cdot}10^{-5}$	24
PU1c	$9.9{\cdot}10^{-5}$	20

formation of hydrogen bonds [31,40], the effect of modifying the synthesis methodology and polyols content on the degree of phase separation and the development of different urethane and urea linkage contributions was encompassed. Upon drawing a baseline in the range 1600–1770 cm^{-1} and locating the overlapped bands through the evaluation of the second-order derivative of the absorbance curves versus wavenumbers [41], an Origin 9.0 Software was used to mathematically decompose the carbonyl region into Gaussian-shape functions. Owing to the variety of proton acceptor functional groups, including C-O-C_{SS}, C═O_{SS} and C═O_{HS}, competing with one another for hydrogen bridging with the urea/urethane N–H proton donor [40], the resulting absorption bands, collected in Table S 2, comprise not only free (1722-1735 cm^{-1}) and disordered (1717 cm^{-1}) and ordered (1698-1705 cm^{-1}) H-bonded urethane carbonyl groups developed during the adhesive synthesis, but also free (1673-1694 cm^{-1}), disordered (1652-1669 cm^{-1}) and ordered (1635-1626 cm^{-1}) H-bonded urea carbonyl groups appearing in the curing step [1,41]. Consequently, as previously reported [42], ordered C═O entities are ascribed to carbonyl groups in hard domains connected to each other, while in disordered carbonyl groups, by contrast, the adjacent N–H groups are associated with the proton acceptor located in the soft segments.

Moreover, an extra absorption band located at 1617 cm^{-1} arises from the amide I range deconvolution assigned to N–H bending vibration for secondary amines [38], originated as a consequence of the moisture-cure in conjunction with the lack of the mobility of the chains due to the progress of the reaction. Thus, highly diluted isocyanate groups in the polymer network may still react with environmental humidity, but their further interaction with additional NCO to produce a urea linkage could be inhibited [41].

In addition, when analysing the advance of the ageing until completion of curing (Fig. 3), some differences can be perceived. A total disappearance of the NCO peak was noticed for all fully cured bio-adhesives while increasing the absorption of the N–H stretching and secondary-amine bending vibration bands (3325 and 1617 cm^{-1}). Besides that, the location of the N–H stretching peak suggests that all these functional groups are hydrogen-bonded to a proton-acceptor entity. Moreover, the absence of some absorption bands, such as N–H bending

at the wavelengths 1336 and 1617 cm^{-1}, at the early curing stages (Fig. 3a), along with the apparent intensity increase in the whole amide I and II ranges, corroborate the assignments previously established.

Furthermore, according to previous investigations [37], the degree of phase separation (DPS) of a block-polyurethane may be determined as the proportion of hydrogen-bonded carbonyl groups resulting from deconvolution of the carbonyl region (eq. 3):

$$DPS = \frac{\sum A_{H-Bond}}{\sum A_{H-Bond} + \sum A_{Free}} \quad (3)$$

where $A_{H\text{-}Bond}$ and A_{Free} are the normalized areas attributable to hydrogen and non-hydrogen bonded C═O in urethane and urea linkages. Figure S 2 shows the deconvoluted bands of the carbonyl functional groups in the amide I region and the proportions of free and hydrogen-bonded urea and urethane contributions obtained from this mathematical procedure are collected in Table 3. As can be observed, when applying the single-step protocol (PU1a), a higher urea/urethane ratio was achieved, owing to the fact that urea production is promoted under longer contact times with the environment (Fig. 2). However, the simplified synthetic route was allowed to reach lower values of DPS meaning a higher soft and hard domains compatibility, which unexpectedly enhanced the ultimate properties, as will be discussed below. Furthermore, when the NCO:OH molar ratio was kept constant (1.87), but castor oil was used as the only OH-source in the bio-based polyurethane production (PU1b vs PU1a), a noticeable rise in urea proportion was noticed, due to the steric hindrance of the secondary OH in the castor oil structure, thus promoting the reaction with environmental H_2O and increasing the degree of phase separation. In an effort to achieve similar performance to the synthesized PU1a adhesive without using CA, the NCO:OH ratio was slightly increased, resulting in a bio-sourced polyurethane adhesive (PU1c) with a greater microphase separation since hydrogen-bonded hard segments impede the segmental motion of the polymer network [43].

3.2. Thermal characterization

The impact of synthesis protocol and the role of CA on the thermal stability of the bio-based PU adhesives studied was explored by applying thermogravimetric analysis. The resulting thermograms and their derivative curves (DTA) are shown in Fig. 4. Firstly, regardless of the synthetic route and CO/CA/HMDI proportions employed, a paltry weight loss (<0.6%) centred at 100 °C was observed, associated with water molecules retained during the curing stage [34].

Owing to the disparate stabilities of both microphases (SS and HS), along with the variable proportions of the reagents, it could be asserted that the synthesized bio-sourced polyurethanes are characterized by a complex thermal decomposition mechanism [44] inasmuch as DTA curves revealed several-step decomposition patterns (Fig. 4b). Furthermore, in previous studies [45] the temperatures at which a 10% mass is lost ($T_{10\%}$) were regarded as the beginning of the decomposition process. Therefore, the main degradation steps were evaluated and analysed in terms of the temperatures for maximum decomposition rate (T_{Max}), the onset and final temperatures (T_{Onset} and T_{Final}) of each step, together with the corresponding $T_{10\%}$ and the final char residue (R) (Table 4).

Table 3
Deconvolution results in terms of percentages of the different contributions in the C═O region.

Sample		PU2	PU1a	PU1b	PU1c
Urethane	**Free**	13.67	27.85	18.74	9.03
	H-bond	54.20	24.16	31.76	36.79
Urea	**Free**	11.96	23.62	26.08	26.95
	H-bond	20.17	24.37	23.41	27.23
Urea/urethane		0.47	0.92	0.98	1.18
DPS		0.74	0.49	0.55	0.64

Disregarding free water removal, most of the polyurethanes, except for PU1b, decomposed in two steps, where the first thermal event (342–365C) was associated with the hard segment domains, while the following peak (459–463 °C) may be ascribed to soft segment backbones, i.e., the cleavage of the C–C bonds [46,47]. The natural-based adhesive PU1b sample, however, presents a main peak in the range from 322 up to 479 °C coupled with an apparent small shoulder at around 459 °C, unambiguously attributed to carbon-to-carbon scission.

On the other hand, some overlapping can be noticed in the temperature range of 300–450 °C, due to the proximity of the decomposition steps of hard and soft segments domains, which impedes the identification of the weight loss for each event. Moreover, in most PU systems, two slight shoulders appeared at 380 and 394–425 °C, likely attributed to the HS entities [37] and the castor oil [4,48] degradation, respectively. The appearance of several decomposition ranges assigned to the hard segment phase emerges on account of the polyurethane synthesis conditions, which promotes the production of hard segment domains, comprising urethane and urea linkages, with a varying degree of organizational order [49].

As can be noticed from the TGA results, simplification of the synthesis protocol seemed to produce no impact on the thermal stability of the synthesized bio-based polyurethanes (PU2 vs PU1a). However, cellulose acetate removal from the adhesive formulation (PU1b and PU1c) led to a shift of 20 °C in the second decomposition step assigned to hard domains (364 °C), due to the fact that, according to previous research [29], the maximum decomposition rate of cellulose acetate (T_{Max}) is attained at 358 °C, while suffering no detrimental effect on thermal stability ($T_{10\%}$). Moreover, the increase of castor oil content in the natural adhesive PU1b aimed to maintain the NCO:OH ratio at 1.87, resulted in an overlap of the degradation steps attributed to the natural oil and C–C splitting (Fig. 4b). When the oil content was once again reduced, thereby increasing the NCO:OH ratio (PU1c), the peak linked to C–C disruption could be differentiated, increasing the intensity of the peak associated to HS units and shifting the CO decomposition shoulder to lower temperatures.

The structure of the synthesized natural bio-adhesives was further analysed by means of DSC experiments. Fig. 5a illustrates the standard calorimetric results obtained in the temperature range from −80 up to 300 °C. As can be inferred, the main thermal transitions identified for all PU adhesives comprise two glass transition temperatures (related to both soft and hard phases, T_g^{SS} and T_g^{HS}), an exothermic event followed by an endothermic peak. For comparative purposes in segmented polyurethanes, the location of the glass transition temperatures (T_gs) has been largely considered as an indicative value to assess the degree of phase separation [10], since T_gs are strongly influenced by the phase miscibility so that the greater values of T_g^{SS}, the lower DPS as a consequence of tougher interaction between both microdomains. Therefore, comparing the natural polyurethanes PU2 and PU1a, regarding the synthesis protocol modification, an apparent reduction in the glass transition temperature difference of both segments was observed, thus evincing the enhancement of the microphase compatibility owing to the increase in the urea linkage production when implementing the straight through synthetic route, in agreement with the FTIR results. Furthermore, when replacing cellulose acetate with additional castor oil, despite the fact that the NCO:OH ratio remained unchanged, CO weight percentage increased by 10%, leading to a reduction in the T_g^{SS}, notwithstanding the DPS values (see Table 3). Afterwards, when raising the HMDI content (PU1c), higher phase separation was obtained, also according to spectroscopic results, thus increasing the T_g^{SS} value, since a higher amount of aggregates of rigid units are more widely distributed in the soft phase, thus hindering the polymer chains mobility [50].

On the other hand, the exothermic peak located in the range of 130–250 °C, whose onset ($T_{Onset,TA}$) and maximum ($T_{Max,TA}$) temperatures can be found in Table 5, may be generally associated with different

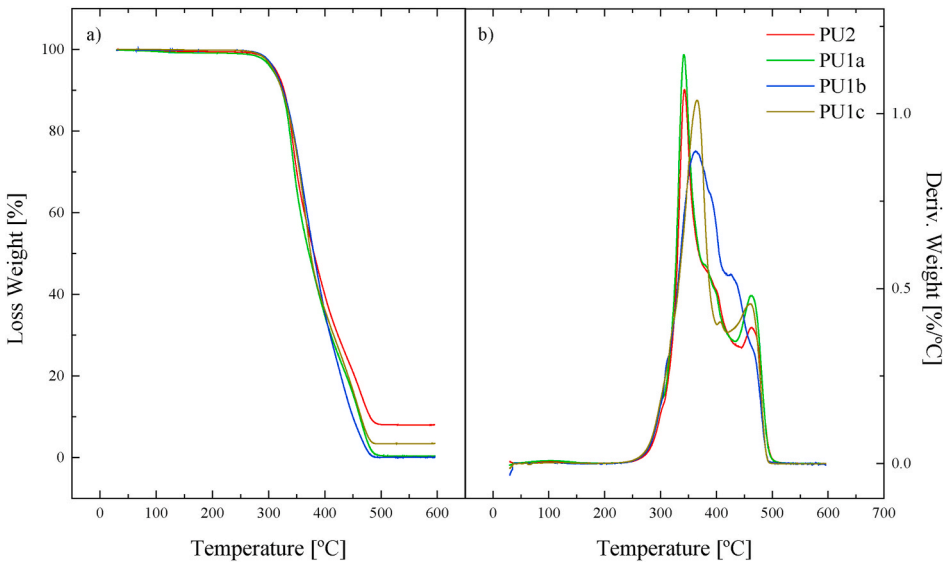

Fig. 4. Loss weight thermograms (a) and corresponding derivative curves (b) for the different bio-based PU formulations studied.

Table 4
Thermal decomposition steps' parameters obtained from thermogravimetric analysis.

Sample	$T_{10\%}$ [°C]	T_{Onset} [°C]	T_{Max} [°C]	T_{Final} [°C]	R [%]
PU2	327	72/322/454	114/343/463	150/413/484	8.01
PU1a	324	55/321/449	105/342/462	143/409/482	0.38
PU1b	326	32/322	90/363	104/479	3.6
PU1c	324	30/326/443	93/365/460	128/411/479	3.4

transitions implying an energy release due to curing steps, crystallization, or other irreversible chain rearrangements. However, in this case, since PU adhesives were fully cured, this event may be related to either crystallization or rearrangement processes of the polymer chains, through which a more ordered polymer network may be obtained. In this sense, PU materials encompass a wide array of polymers, ranging from semicrystalline [37] to totally amorphous structures [47]. Nevertheless, polyurethanes sometimes present a certain degree of organization, which should not be regarded as crystallites as such, but more ordered domains [40]. As previously pointed out by Refs. [51,52] at those temperatures, a typical thermal rearrangement of the disordered HS entities takes place. Regarding the energy associated with this thermal rearrangement ($\Delta H_{Annealing}$), it apparently remains constant when the traditional protocol was substituted with the single-step procedure, despite showing a greater phase mixing. Nevertheless, the higher flexibility and length of the fatty acid chains in castor oil facilitated the chain annealing in bio-sourced adhesive PU1b. This effect was mitigated when increasing the NCO:OH molar ratio, so that a higher content of hard segment, acting as crosslinking points, could hamper the molecular mobility, thus reducing the released energy during the thermal annealing (Table 5).

Finally, the last thermal transition involved an endothermic peak whose minimum temperatures were found in the range of 283–288 °C, which may be ascribed to a melting of the likely crystalline region of the polyurethanes or polyurethane decomposition [53,54]. Aiming to clarify the nature of this event, in addition to identify overlapping of different thermal events in block-polyurethanes, temperature modulated differential scanning calorimetry (MDSC) analysis was performed over all bio-sourced adhesives in the range from 0 up to 300 °C. Fig. 5b shows selected MDSC results for PU2 adhesive. In all the cases, a similar behaviour was obtained, so that at around 280 °C an endothermic peak was observed in the non-reversing heat flow curve. Subsequently, taking

Table 5
Characteristic parameters associated with thermal events exhibited by bio-sourced PUs during DSC analyses.

Sample	$T_{g,SS}$ [°C]	$T_{g,HS}$ [°C]	$\Delta H_{Annealing}$ [J/g]	$T_{Onset,TA}$ [°C]	$T_{Max,TA}$ [°C]	$T_{Decomp.}$ [°C]
PU2	−20.7	52.0	12.5	162.8	198.1	283.3
PU1a	−16.8	48.7	10.2	190.9	215.8	284.4
PU1b	−20.2	51.6	20.3	140.6	183.5	288.6
PU1c	−16.8	47.7	11.1	181.0	204.3	284.7

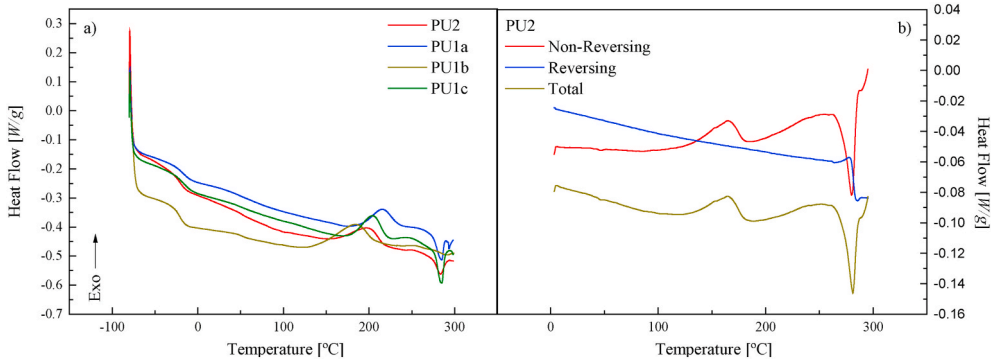

Fig. 5. DSC curves for all bio-based PU adhesives (a) and curves from modulated temperature DSC test for a selected sample (PU2) (b).

into consideration that most of the melting transitions appear in the reversing curve, along with the fact that, according to the TGA results (Fig. 4), on average 1.2% of weight is lost at 280 °C, this peak must be undoubtedly assigned to a thermal decomposition, instead of a melting process [55]. Consequently, the previous exothermic peak is also attributed to the rearrangement of the polymer chains, instead of a crystallization, since no melting transition of those crystallites was obtained.

3.3. Rheology

The rheological response of the synthesized bio-inspired adhesives under torsional mode was evaluated after completion of the curing process and benchmarked against selected commercial references. Thus, Fig. 6 shows the influence of temperature on the evolution of the storage moduli and loss tangent at 1 Hz, when a temperature ramp from 25 to 200 °C is applied at a heating rate of 2 °C/min. As in other similar bio-adhesive formulations previously developed using aromatic diisocyanates [56], an eminently elastic response was observed over the whole temperature range studied, where the tanδ values remained always lower than one, and also lower than those values exhibited by the reference benchmarks.

Generally, the temperature seems to exert a slight influence on the bio-based adhesives' storage moduli, which levelled off till a critical value of around 80–120 °C, depending on the preparation method and the inclusion of cellulose acetate in the formulation. Thus, samples containing cellulose acetate in their composition show good thermal stability up to temperature values around 80–100 °C. However, when comparing samples PU1b and PU1c (without cellulose acetate), the temperature dependence of these samples is significantly different, especially when analysing the evolution of the loss tangent. Thus, the elastic component of the bio-adhesive that does not contain the biopolymer but the same NCO:OH ratio (PU1b) has a slightly lower thermal stability compared to that containing cellulose acetate, but the influence of temperature is much more pronounced in the tanδ (Fig. 6b). The same evolution is exhibited by the sample containing a higher NCO:OH ratio (PU1c). These results support those obtained from TGA tests, which concluded that the protocol simplification seemed to produce no impact on the thermal stability of the synthesized bio-based polyurethanes (PU2 vs PU1a). However, cellulose acetate removal from the adhesive formulation (PU1b and PU1c) led to a significant decrease in the SAOS functions and higher thermal dependence in the viscous component, especially above 120 °C. Moreover, despite the similar or larger (particularly at high temperature for sample C.Ad.2) values of the elastic moduli exhibited by the benchmark references, as previously mentioned, the prepared bio-sourced polyurethanes have shown a significantly higher relative elasticity, mainly noticeable in the loss tangent, around one order of magnitude lower than those found in commercial adhesives (Fig. 6b).

Fig. 7 shows the evolution of viscoelastic moduli (G′, G″ and tan δ) with frequency as a function of the preparation protocol and CA addition, at selected temperatures (25, 80 and 150 °C). As can be noticed, G' values are much higher than those found for G″, and hardly influenced by the frequency, thus showing a well-developed plateau region of the mechanical spectrum. This behaviour is independent of the temperature and again characterized by a predominant elastic behaviour throughout the whole frequency range analysed. Although the most important effect of temperature in bio-based PUs is a clear change in G″ frequency dependence at temperatures higher than 60 °C, both viscoelastic functions appear to decline unfailingly with temperature for the commercial benchmark C.Ad.1, while for C.Ad.2 this remains more thermally unaffected (see Fig. 7b, e). Despite this, bio-sourced PU adhesives are characterized by elastic moduli within the range associated with the commercial benchmarks, but with a noticeably higher relative elasticity (Fig. 7c,f,i) as a consequence of the lower values of G" generally found.

On the other hand, the lower values of the viscoelastic moduli shown by the CA-free sample (PU1b), despite the higher relative elasticity (lower values of the loss tangent) (Fig. 7c), reflects the reinforcing effect of cellulose acetate on the structure. Additionally, such an impact is also encouraged by the application of the single-step preparation protocol, as noticeable in the viscoelastic functions increase exhibited by sample PU1a in relation to bio-based adhesive PU2. Similar results have been previously obtained when studying the effect of cellulosic derivatives on the microstructure and thermomechanical properties of other bio-based polyurethane systems [57,58].

With the aim of unifying the temperature dependence of the synthesized formulations, the time-temperature (t-T) superposition principle was applied, from 25 to 110 °C, by superimposing the above-mentioned viscoelastic functions with the aid of appropriate shift factors, a_T, taking 25 °C as the reference temperature. As can be inferred

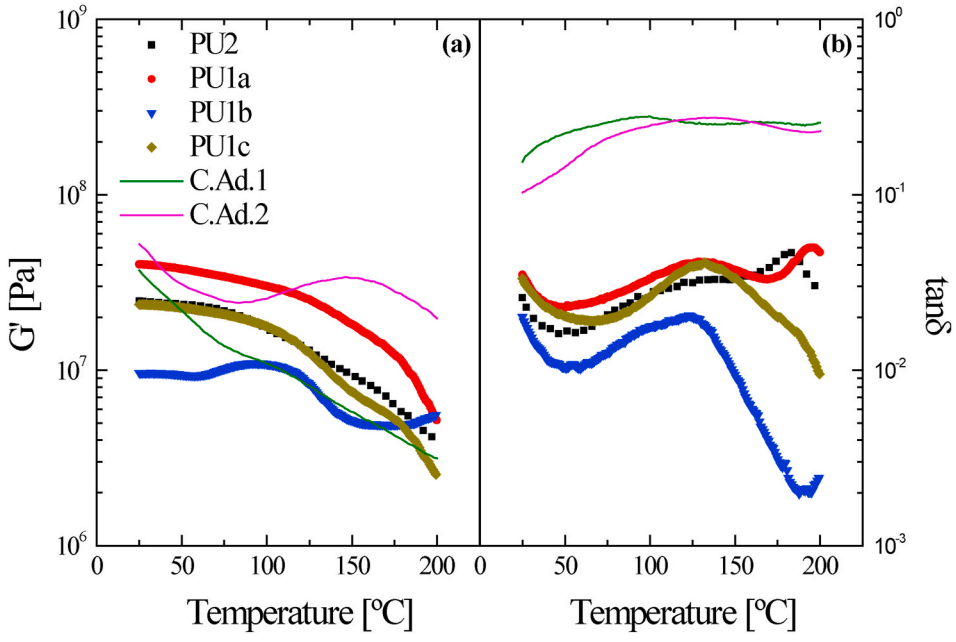

Fig. 6. Evolution of the linear elastic moduli (a) and loss tangent (b) with temperature during the application of an upward temperature ramp of 2 °C/min.

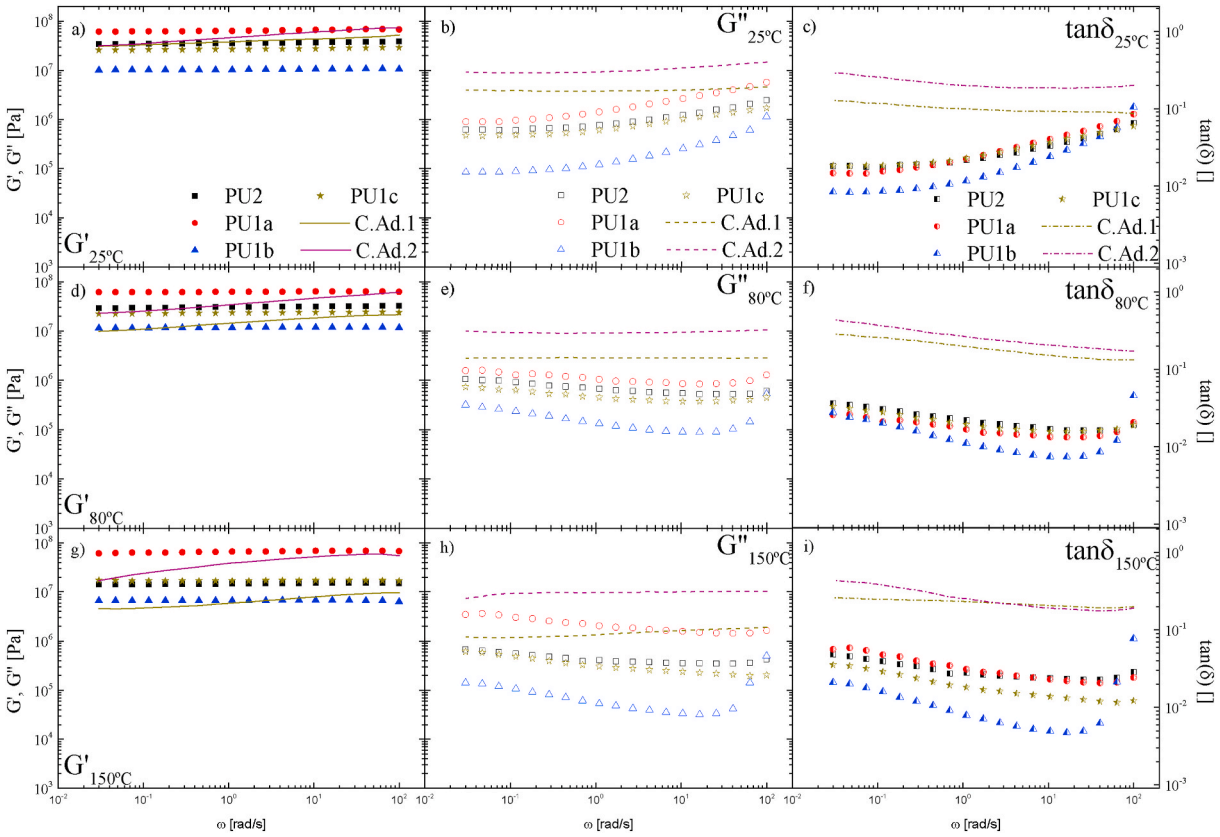

Fig. 7. Frequency sweep dependence of (a, d, g) G′, (b, e, h) G″ and (c, f, i) tanδ at selected temperatures (25, 80 and 150 °C) of all PU adhesives.

from Fig. 8, the t-T superposition principle can only be successfully applied up to a temperature of around 110–130 °C, definitely failing above 150 °C, which again suggests a temperature-induced change in structural arrangement, as previously discussed in DSC analysis (Table 5). Unlike previously reported results devoted to the preparation of aromatic diisocyanate-based polyurethane adhesives [56], the applicability of the t-T superposition principle is not restrained by the functionalization degree (NCO:OH ratio) or, in this case, by the addition of cellulose acetate and the synthesis protocol, likely as a result of the improved compatibility between hard and soft segments arising from the aliphatic nature of the diisocyanate (HMDI) as well as the vegetable oil utilized in this research. The resulting shift factors for all systems have been fitted to the Williams-Landel-Ferry (WLF) model (inside Fig. 8).

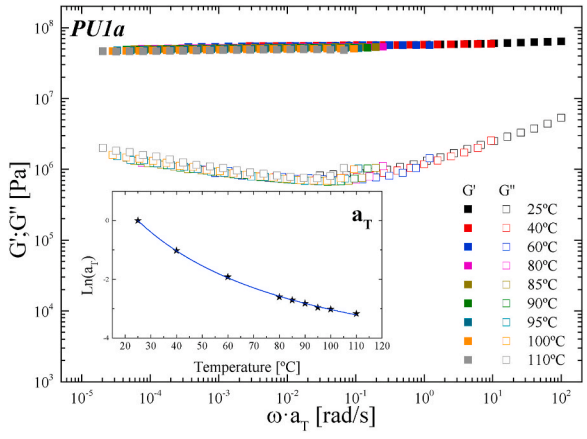

Fig. 8. Time-temperature superposition for a selected formulation (PU1a) and fitting of the corresponding shift factors to the William-Landel-Ferry equation (inside).

$$log(a_T) = \frac{-C_1 \cdot (T - T_{Ref})}{C_2 + (T - T_{Ref})} \quad (4)$$

where C_1 and C_2, are the constant parameters of the WLF model, T is the temperature and T_{Ref} is the reference temperature (25 °C). The parameters resulting from the fitting are gathered in Table 6.

As can be deduced from Table 6, these fitting parameters show the same evolution as the T_g^{SS} when analysing the effect of the synthesis protocol as well as the reagent proportions. Therefore, attending to Equation (4), higher values of parameters C_1 and C_2 entail, for a given temperature increment, a higher reduction in the shift factor, meaning a more pronounced thermal susceptibility. Thus, elastomers PU1a and PU1c showed a noticeably lower influence of temperature on the SAOS functions, thus diminishing the frequency range attainable with the application of the t-T superposition principle.

3.4. Adhesion performance

The adhesion response of an adhesive is, according to Baldan [59], the resistance to the debonding process of an adhesive joint, arising from an array of adhesion phenomena, which may comprise interactions of rheological, physical, chemical and mechanical nature. However, more

Table 6
Williams-Landel-Ferry fitting parameters.

Sample	C_1	C_2 [K]
PU2	10.93	146.71
PU1a	5.87	70.41
PU1b	11.10	148.27
PU1c	5.85	68.09

specifically, when considering wood as a substrate, in terms of the surface nature, chemical interaction and mechanical interlocking appear to be the most likely adhesion phenomena. Therefore, the adhesion performance of the adhesives on different wooden substrates was assessed by using the applicable ASTM tests for peeling strength, conventionally expressed as the force per unit width (ASTM D903) and shear strength (ASTM D906 for wood). Table 7 collects the shear and peeling strength values for the different bio-adhesives and commercial systems on various types of wood substrates (poplar, spruce, plywood, DMF and oakwood). For benchmarking purposes and more specifically regarding the synthetic route, the reference systems C.Ad.1, C.Ad.2 and the bio-polyurethane manufactured using the two-stage protocol were tested only on poplar wood, while when assessing the inclusion of cellulose acetate and the HMDI:CO ratio, the adhesion analysis was extended to other wooden substrates (plywood, medium-density fibreboard, spruce wood and oak wood). As a general rule, regardless of the synthetic route, the adhesion response of bio-based polyurethanes seems to exceed commercial benchmarks under shear as well as peeling deformation. Indeed, although the cellulose acetate-free adhesive prepared using the simplified protocol (PU1b) is the one with the lowest shear and peeling strengths in most wooden substrates, its shear strength on poplar wood become above 50 and 17% higher than the 2.5 and 3.2 MPa found for benchmarks C.Ad.1 and C.Ad.2, respectively [30]. Consequently, as can be noticed, the structural reinforcing action of cellulose acetate is evidenced. Moreover, regardless of either the addition of cellulose derivative or the NCO: OH ratio, the simplified one-step synthesis procedure provided natural polyurethane adhesives whose shear strengths can't be significantly differentiated with each other considering the results obtained by ANOVA statistical tests with a 5% of significance level (see Supporting Information), despite the slight reduction in peeling strength. However, the adhesive manufactured with a higher NCO:OH ratio and free of cellulose acetate (PU1c), along with the formulation PU1a, had remarkable shear strength values on oak wood. In general, the higher adhesion performance found with PU1c must be attributed to the effect of the NCO:OH ratio on the mechanical properties of the adhesives, which in turn is similar to the CA reinforcing effect found with sample PU1a.

Regarding the types of failure provided by polyurethanes adhesives synthesized through the single-step protocol, except for the adhesion performance on oak wood in which a mixture of adhesive and cohesive failure was obtained, the failure is predominantly located within the substrate. This seems to be a more appropriate and desirable sort of failure inasmuch as it entails that these PU-adhesives exhibit superior mechanical resistance in comparison with their corresponding adhesion substrate. Thus, even though the adhesion strengths under shear deformation are not statistically different when conducting the bio-sourced adhesive synthesis via the proposed single-step process, the failure becomes mainly substrate-based, so that the adhesion performance is clearly enhanced. Moreover, the values of the lap shear strength provided by the ASTM D906 test obtained with the synthesized PUs, particularly noticeable on oak wood, seem to meet the requirements for being considered as wood adhesives, since they appear to be fairly competitive with the values previously reported by Silva et al. [60], Ang et al. [61] and Sahoo et al. [14], even exceeding those resulting from the investigations of Somani et al. [62], Patel et al. [28] or Wang et al. [63], thus encompassing a wide range of polyurethane adhesives, most of them based on castor oil and both aromatic and aliphatic diisocyanates.

In relation to the peeling tests, besides exceeding the adhesion resistances provided by commercial benchmarks C.Ad.1 (2.2 kN/m) and C.Ad.2 (0.9 kN/m) [30], once again the synthesized bio-adhesive prepared with the simplified one-step protocol and without cellulose acetate is the one that shows lower peeling strength values in all types of substrate; while the rest of the adhesives present values very close to those obtained with the polyurethane manufactured in two stages containing cellulose acetate. In agreement with thermal and rheological results, bio-based adhesives PU1a and PU1c showed a similar adhesive response, with peeling strengths statistically similar (see Supporting Information). Finally, regarding the type of failure, in most of the cases, the failure in peeling tests is mainly located in the interphase adhesive-substrate, with the exception of the system PU1c which, probably owing to the greater NCO:OH ratio, evidenced a significant substrate failure contribution at break (70–85% of the failure).

Table 7
Adhesion strengths developed by PU systems under shear and peeling deformation.

Tests		PU2	PU1a	PU1b	PU1c
Shear Strengths [MPa]	PW	3.321 ± 0.054^{a,b,c}	4.297 ± 1.082^{c}	3.773 ± 0.546^{a,c}	4.422 ± 1.076^{c}
	PlyW	–	1.523 ± 0.311^{c}	1.706 ± 0.183^{c}	1.726 ± 0.288^{c}
	MDF	–	1.633 ± 0.204^{c}	1.861 ± 0.474^{c}	1.845 ± 0.537^{c}
	SW	–	0.847 ± 0.001^{c}	0.974 ± 0.215^{c}	0.854 ± 0.159^{c}
	OW	–	5.308 ± 0.489^{a,b}	3.154 ± 0.153^{a,b}	6.039 ± 0.716^{a,b}
Peeling Strengths [kN/m]	PW	3.243 ± 0.194^{b}	2.643 ± 0.045^{b}	2.278 ± 0.303^{b}	2.021 ± 0.411^{b}
	PlyW	–	3.383 ± 0.190^{a,b}	2.064 ± 0.411^{a,b}	4.706 ± 0.368^{b,c}
	MDF	–	3.435 ± 0.672^{a,b}	1.952 ± 0.494^{a,b}	3.241 ± 1.131^{a,b,c}
	SW	–	3.070 ± 0.456^{a}	2.381 ± 0.348^{a,b}	3.159 ± 0.388^{a}
	OW	–	3.438 ± 0.175^{a,c}	1.956 ± 0.504^{a,b}	2.826 ± 0.573^{a,c}

Failures: [a] Cohesion; [b] Adhesion; [c] Substrate.

4. Conclusions

In this study, a new synthetic solvent-free route for the production of bio-inspired polyurethane adhesives conforming the tenets of the green chemistry was properly addressed, and the resulting vegetable oil-based adhesives were compared to commercial benchmarks and those obtained via a traditional solvent-borne protocol. This investigation also encompasses the impact of the reagents content, namely cellulose acetate, castor oil and 1,6-hexamethylene diisocyanate, on the ultimate adhesion properties. Thus, following the simplified one-step solvent-free processing protocol and the addition of cellulose acetate led to shorter moisture-curing steps and reinforced polymer networks with higher values of viscoelastic moduli and lower thermal dependence of the rheological functions. Furthermore, rheological results revealed a sharp elastomeric response, characterised by the rubbery region of the mechanical spectrum, within extensive temperature and frequency ranges. The application of the time-temperature superposition principle was solely limited by a critical temperature (of around 110–125 °C), as a result of the temperature-induced structural rearrangements. Moreover, the complex nature of the bio-polyurethane chemical structure consisting of soft and hard segments and inter- and intra-domain hydrogen bonding, thus developing regions with different degrees of order, was identified from the thermal and spectroscopic results, in good agreement with the appearance of two glass transition temperatures and exothermic thermal rearrangement. In this connection, the proposed single-step procedure fostered microphase mixing, yielding reduced DPS and increasing T_g^{SS} accordingly. At the same time the straight-through method allowed for the achievement of statistically indistinguishable shear strengths, always higher than those provided by the selected commercial adhesives and with a much more appealing sort of failure located in the substrate through a cleaner and simpler approach, despite exhibiting similar thermal stability ($T_{10\%}$) and peeling resistance.

Declaration of competing interest

The authors declare no conflict of interest.

Acknowledgements

Funding: This work is part of two research projects (CTQ2014–56038-C3-1R and TEP-1499) sponsored by MINECO-FEDER and Junta de Andalucía programmes, respectively. One of the authors (Adrián Tenorio-Alfonso) has also received a PhD. Research Grant from "Ministerio de Educación" (FPU13/01114). Funding for open access charge was provided by Universidad de Huelva / CBUA. The authors gratefully acknowledge the financial support.

Appendix A. Supplementary data

Supplementary data to this article can be found online at https://doi.org/10.1016/j.ijadhadh.2022.103153.

References

[1] Otorgust G, Dodiuk H, Kenig S, Tenne R. Important insights into polyurethane nanocomposite-adhesives; a comparative study between INT-WS 2 and CNT. Eur Polym J 2017;89:281–300.
[2] Casdorff K, Kläusler O, Gabriel J, Amen C, Lehringer C, Burgert I, Keplinger T. About the influence of a water-based priming system on the interactions between wood and one-component polyurethane adhesive studied by atomic force microscopy and confocal Raman spectroscopy imaging. Int J Adhesion Adhes 2018;80:52–9.
[3] Market Study. Adhesives - World 3rd Edition. Available online: https://www.ceresana.com/en. [Accessed 16 December 2019].
[4] Liu K, Miao S, Su Z, Sun L, Ma G, Zhang S. Castor oil-based waterborne polyurethanes with tunable properties and excellent biocompatibility. Eur J Lipid Sci Technol 2016;118:1512–20.
[5] Moghadam PN, Yarmohamadi M, Hasanzadeh R, Nuri S. Preparation of polyurethane wood adhesives by polyols formulated with polyester polyols based on castor oil. Int J Adhesion Adhes 2016;68:273–82.
[6] Clerc G, Brülisauer M, Affolter S, Volkmer T, Pichelin F, Niemz P. Characterization of the ageing process of one-component polyurethane moisture curing wood adhesive. Int J Adhesion Adhes 2017;72:130–8.
[7] Abdolhosseini F, Givi MKB. Characterization of a biodegradable polyurethane elastomer derived from castor oil. Am J Polym Sci 2016;6:18–27.
[8] Calvo-Correas T, Martin MD, Retegi A, Gabilondo N, Corcuera MA, Eceiza A. Synthesis and characterization of polyurethanes with high renewable carbon content and tailored properties. ACS Sustainable Chem Eng 2016;4:5684–92.
[9] Norhisham SM, Maznee TTN, Ain HN, Devi PK, Srihanum A, Norhayati MN, Yeong SK, Hazimah AH, Schiffman CM, Sendijarevic A. Soft polyurethane elastomers with adhesion properties based on palm olein and palm oil fatty acid methyl ester polyols. Int J Adhesion Adhes 2017;73:38–44.
[10] Güney A, Hasirci N. Properties and phase segregation of crosslinked PCL-based polyurethanes. J Appl Polym Sci 2014;131:1–13.
[11] Yilgör E, Burgaz E, Yurtsever E, Yilgör I. Comparison of hydrogen bonding in polydimethylsiloxane and polyether based urethane and urea copolymers. Polymer 2000;41:849–57.
[12] Cui S, Luo X, Li Y. Synthesis and properties of polyurethane wood adhesives derived from crude glycerol-based polyols. Int J Adhesion Adhes 2017;79:67–72.
[13] Oprea S, Potolinca VO, Gradinariu P, Joga A, Oprea V. Synthesis, properties, and fungal degradation of castor-oil-based polyurethane composites with different cellulose contents. Cellulose 2016;23:2515–26.
[14] Sahoo S, Kalita H, Mohanty S, Nayak SK. Synthesis and characterization of vegetable oil based polyurethane derived from low viscous bio aliphatic isocyanate: adhesion strength to wood-wood substrate bonding. Macromol Res 2017;25:1–7.
[15] Liu H, Li C, Sun XS. Soy-oil-based waterborne polyurethane improved wet strength of soy protein adhesives on wood. Int J Adhesion Adhes 2017;73:66–74.
[16] Mishra D, Sinha VK. Eco-economical polyurethane wood adhesives from cellulosic waste: synthesis, characterization and adhesion study. Int J Adhesion Adhes 2010;30:47–54.
[17] Cui S, Liu Z, Li Y. Bio-polyols synthesized from crude glycerol and applications on polyurethane wood adhesives. Ind Crop Prod 2017;108:798–805.
[18] Santamaria-Echart A, Ugarte L, García-Astrain C, Arbelaiz A, Corcuera MA, Eceiza A. Cellulose nanocrystals reinforced environmentally-friendly waterborne polyurethane nanocomposites. Carbohydr Polym 2016;151:1203–9.
[19] Zain NM, Roslin EN, Ahmad S. Preliminary study on bio-based polyurethane adhesive/aluminum laminated composites for automotive applications. Int J Adhesion Adhes 2016;71:1–9.
[20] Alagi P, Ghorpade R, Jang JH, Patil C, Jirimali H, Gite V, Hong SC. Functional soybean oil-based polyols as sustainable feedstocks for polyurethane coatings. Ind Crop Prod 2018;113:249–58.
[21] Datta J, Głowińska E. Effect of hydroxylated soybean oil and bio-based propanediol on the structure and thermal properties of synthesized bio-polyurethanes. Ind Crop Prod 2014;61:84–91.
[22] Aung MM, Yaakob Z, Kamarudin S, Abdullah LC. Synthesis and characterization of Jatropha (Jatropha curcas L.) oil-based polyurethane wood adhesive. Ind Crop Prod 2014;60:177–85.
[23] Fiorelli J, Curtolo DD, Barrero NG, Savastano Jr H, Pallone Eliria, Maria de Jesus Agnolon, Johnson R. Particulate composite based on coconut fiber and castor oil polyurethane adhesive: an eco-efficient product. Ind Crop Prod 2012;40:69–75.
[24] Allauddin S, Narayan R, Raju K. Synthesis and properties of alkoxysilane castor oil and their polyurethane/urea–silica hybrid coating films. ACS Sustainable Chem Eng 2013;1:910–8.
[25] Raghunanan LC, Martínez I, Valencia C, Sánchez MC, Franco JM. Unexpected selectivity in the functionalization of neat castor oil under benign catalyst-free conditions. ACS Sustainable Chem Eng 2018;6:7212–5.
[26] Valero MF, Gonzalez A. Polyurethane adhesive system from castor oil modified by a transesterification reaction. J Elastomers Plastics 2012;44:433–42.
[27] Fonseca LR, Bergman JA, Kessler MR, Madbouly SA, Lima-Neto BS. Self-metathesis of 10-undecen-1-ol with Ru-amine-based complex for preparing the soft segment and chain extender of novel castor oil-based polyurethanes, Macromolecular Symposia. Wiley Online Library; 2016. p. 30–9.
[28] Patel MR, Shukla JM, Patel NK, Patel KH. Biomaterial based novel polyurethane adhesives for wood to wood and metal to metal bonding. Mater Res 2009;12:385–93.
[29] Tenorio-Alfonso A, Sánchez MC, Franco JM. Preparation, characterization and mechanical properties of bio-based polyurethane adhesives from isocyanate-functionalized cellulose acetate and castor oil for bonding wood. Polymers 2017;9:132–45.
[30] Tenorio-Alfonso A, Pizarro ML, Sánchez MC, Franco JM. Assessing the rheological properties and adhesion performance on different substrates of a novel green polyurethane based on castor oil and cellulose acetate: a comparison with commercial adhesives. Int J Adhesion Adhes 2018;82:21–6.
[31] Mekewi MA, Ramadan AM, ElDarse FM, Rehim MHA, Mosa NA, Ibrahim MA. Preparation and characterization of polyurethane plasticizer for flexible packaging applications: natural oils affirmed access. Egypt. J. Petrol. 2017;26:9–15.
[32] Dubé MA, Salehpour S. Applying the principles of green chemistry to polymer production technology. Macromol React Eng 2014;8:7–28.
[33] Cornille A, Michaud G, Simon F, Fouquay S, Auvergne R, Boutevin B, Caillol S. Promising mechanical and adhesive properties of isocyanate-free poly (hydroxyurethane). Eur Polym J 2016;84:404–20.
[34] Kupka V, Vojtova L, Fohlerova Z, Jancar J. Solvent free synthesis and structural evaluation of polyurethane films based on poly (ethylene glycol) and poly (caprolactone). Express Polym Lett 2016;10:479–92.
[35] Raghunanan LC, Fernandez-Prieto S, Martínez I, Valencia C, Sánchez MC, Franco JM. Molecular insights into the mechanisms of humidity-induced changes on the bulk performance of model castor oil derived polyurethane adhesives. Eur Polym J 2018;101:291–303.
[36] Thomas LC. Modulated DSC® paper# 3 modulated DSC® basics; optimization of MDSC® experimental conditions. Technical report. TA Instruments 2005:1–10.
[37] Zieleniewska M, Auguścik M, Prociak A, Rojek P, Ryszkowska J. Polyurethane-urea substrates from rapeseed oil-based polyol for bone tissue cultures intended for application in tissue engineering. Polym Degrad Stabil 2014;108:241–9.
[38] Stuart BH. Organic molecules. In: Ando DJ, editor. Infrared spectroscopy: fundamentals and applications, university of technology. Sidney, Australia: Wiley Online Library; 2004. p. 71–93.
[39] Kantheti S, Narayan R, Raju K. Development of moisture cure polyurethane–urea coatings using 1, 2, 3-triazole core hyperbranched polyesters. J Coating Technol Res 2013;10:609–19.
[40] Mattia J, Painter P. A comparison of hydrogen bonding and order in a polyurethane and poly (urethane– urea) and their blends with poly (ethylene glycol). Macromolecules 2007;40:1546–54.
[41] Zimmer B, Nies C, Schmitt C, Possart W. Chemistry, polymer dynamics and mechanical properties of a two-part polyurethane elastomer during and after crosslinking. Part I: dry conditions. Polymer 2017;115:77–95.
[42] Huacuja-Sánchez JE, Müller K, Possart W. Water diffusion in a crosslinked polyether-based polyurethane adhesive. Int J Adhesion Adhes 2016;66:167–75.
[43] Ayres E, Oréfice RL, Yoshida MI. Phase morphology of hydrolysable polyurethanes derived from aqueous dispersions. Eur Polym J 2007;43:3510–21.
[44] Fuensanta M, Jofre-Reche JA, Rodríguez-Llansola F, Costa V, Iglesias JI, Martín-Martínez JM. Structural characterization of polyurethane ureas and waterborne polyurethane urea dispersions made with mixtures of polyester polyol and polycarbonate diol. Prog Org Coating 2017;112:141–52.
[45] Yakushin V, Stirna U, Bikovens O, Misane M, Sevastyanova I, Vilsone D. Synthesis and characterization of novel polyurethanes based on tall oil. Mater Sci 2013;19:390–6.
[46] Kong X, Zhao L, Curtis JM. Polyurethane nanocomposites incorporating biobased polyols and reinforced with a low fraction of cellulose nanocrystals. Carbohydr Polym 2016;152:487–95.
[47] Puszka A, Kultys A. The influence of soft segments on some properties of new transparent segmented polyurethanes. Polym Adv Technol 2017;28:1937–44.
[48] Zhou Q, Zhang L, Zhang M, Wang B, Wang S. Miscibility, free volume behavior and properties of blends from cellulose acetate and castor oil-based polyurethane. Polymer 2003;44:1733–9.
[49] Alvarez GA, Fuensanta M, Orozco VH, Giraldo LF, Martín-Martínez JM. Hybrid waterborne polyurethane/acrylate dispersion synthesized with bisphenol A-glicidylmethacrylate (Bis-GMA) grafting agent. Prog Org Coating 2018;118:30–9.

[50] Fuensanta M, Martín-Martínez JM. Thermoplastic polyurethane coatings made with mixtures of polyethers of different molecular weights with pressure sensitive adhesion property. Prog Org Coating 2018;118:148–56.
[51] Ning L, De-Ning W, Sheng-Kang Y. Hydrogen-bonding properties of segmented polyether poly (urethane urea) copolymer. Macromolecules 1997;30:4405–9.
[52] Van Ekeren PJ, Carton EP. Polyurethanes for potential use in transparent armour investigated using DSC and DMA. J therm anal calorim 2011;105:591–8.
[53] Cakić SM, Ristić IS, Cincović MM, Nikolić NČ, Nikolić LB, Cvetinov MJ. Synthesis and properties biobased waterborne polyurethanes from glycolysis product of PET waste and poly (caprolactone) diol. Prog Org Coating 2017;105:111–22.
[54] Gurunathan T, Chung JS. Physicochemical oroperties of amino–silane-terminated vegetable oil-based waterborne polyurethane nanocomposites. ACS Sustainable Chem Eng 2016;4:4645–53.
[55] Orgilés-Calpena E, Arán-Aís F, Torró-Palau AM, Orgilés-Barceló C. Biodegradable polyurethane adhesives based on polyols derived from renewable resources. Proc IME J Mater Des Appl 2014;228:125–36.
[56] Tenorio-Alfonso A, Sánchez MC, Franco JM. Synthesis and mechanical properties of bio-sourced polyurethane adhesives obtained from castor oil and MDI-modified cellulose acetate: influence of cellulose acetate modification. Int J Adhesion Adhes 2019:102404.
[57] Gallego R, Arteaga JF, Valencia C, Franco JM. Thickening properties of several NCO-functionalized cellulose derivatives in castor oil. Chem Eng Sci 2015;134:260–8.
[58] Głowińska E, Datta J. Structure, morphology and mechanical behaviour of novel bio-based polyurethane composites with microcrystalline cellulose. Cellulose 2015;22:2471–81.
[59] Baldan A. Adhesion phenomena in bonded joints. Int J Adhesion Adhes 2012;38:95–116.
[60] Silva BB, Santana RM, Forte MM. A solventless castor oil-based PU adhesive for wood and foam substrates. Int J Adhesion Adhes 2010;30:559–65.
[61] Ang KP, Lee CS, Cheng SF, Chuah CH. Synthesis of palm oil-based polyester polyol for polyurethane adhesive production. J Appl Polym Sci 2014;131. 39967 (1)-39967 (8).
[62] Somani KP, Kansara SS, Patel NK, Rakshit AK. Castor oil based polyurethane adhesives for wood-to-wood bonding. Int J Adhesion Adhes 2003;23:269–75.
[63] Wang F, Wang J, Hu L, Chu F, Wang C, Pang J, Cheng Z. Combinations of soy protein and polyacrylate emulsions as wood adhesives. Int J Adhesion Adhes 2018;82:160–5.